



SUPPLEMENTARY MATERIALS

Transport Properties of Cation-Exchange Membranes Obtained by Pore Filling of Track-Etched Membranes with Perfluorosulfonic Acid Polymer

Maria A. Ponomar¹, Veronika V. Sarapulova^{1*}, Vera V. Guliaeva¹,
Pavel Yu. Apel², Natalia D. Pismenskaya¹

¹Kuban State University, Krasnodar, Russia;

²Joint Institute for Nuclear Research, Dubna, Moscow region, Russia

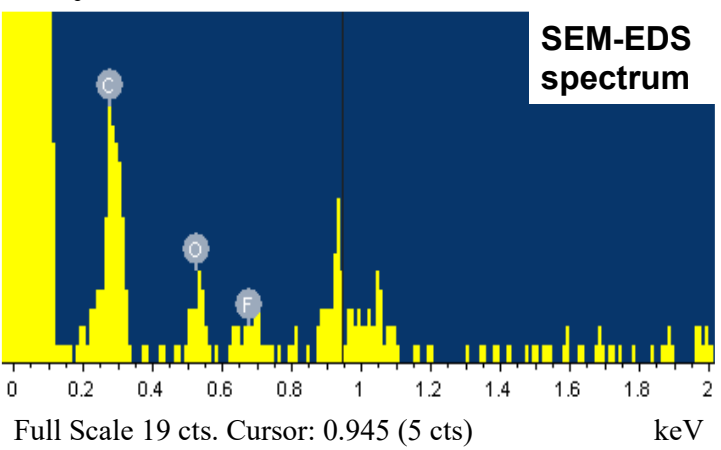
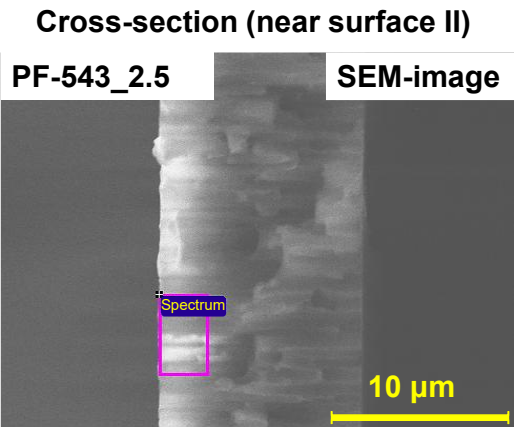
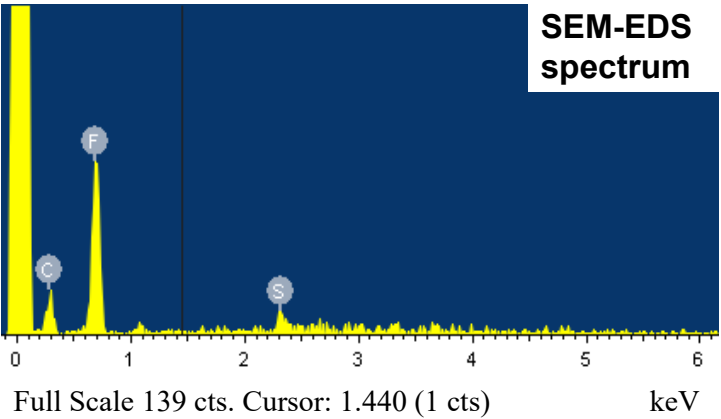
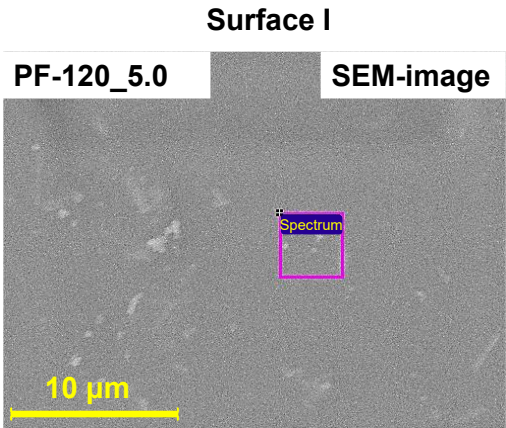
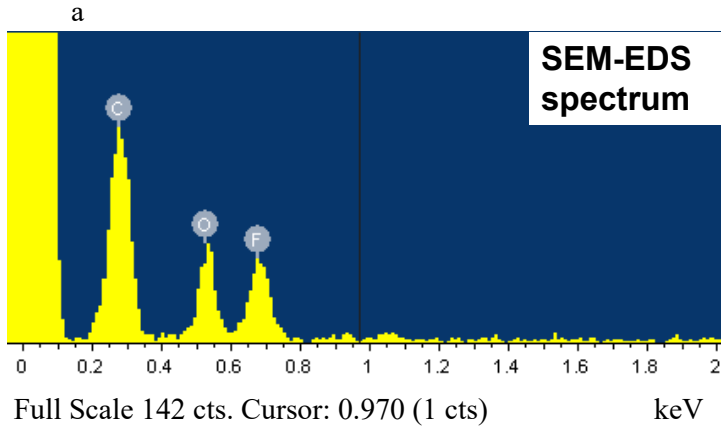
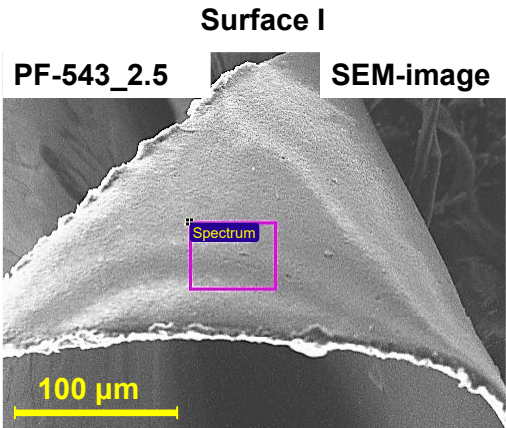
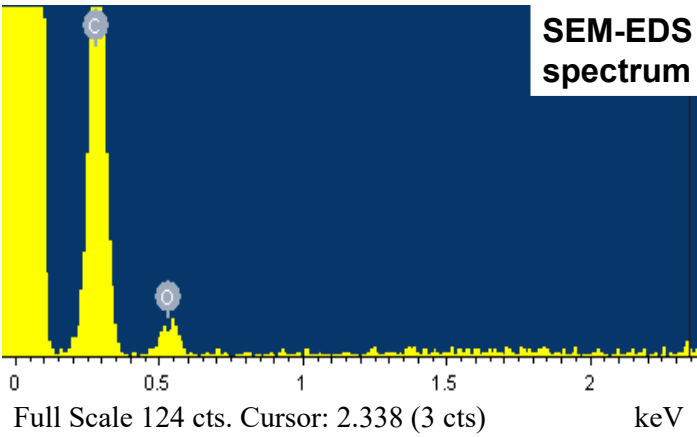
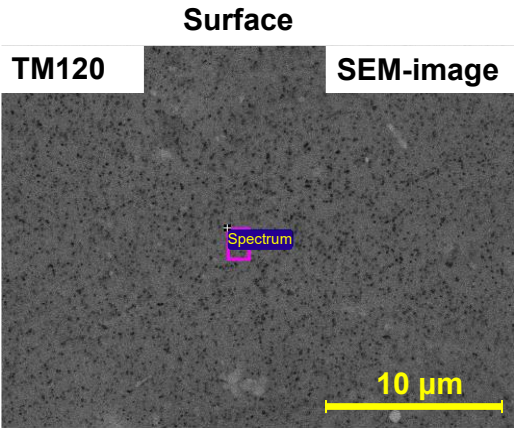
(*Corresponding author's e-mail: vsarapulova@gmail.com)

List of Content

Image of the vacuum filtration device (Figure S1).	S1
SEM-EDS spectrum and SEM images of SEM-EDS analysis areas of the surface TM120 substrate (a), surface I (b,c) and cross-section (near surface II) (d,f) of the experimental sample PF-543_2.5 and PF-120_5 (Figure S2).	S2
A microheterogeneous model algorithm for characterizing membrane structure and transport	S3
Comparison of performances of LF-4SC pore-filled TM membrane PF-543_5 and previously reported different types of commercial and composite membranes fabricated from pore-filling method (Table S1).	S4



Figure S1. Image of the vacuum filtration device



d

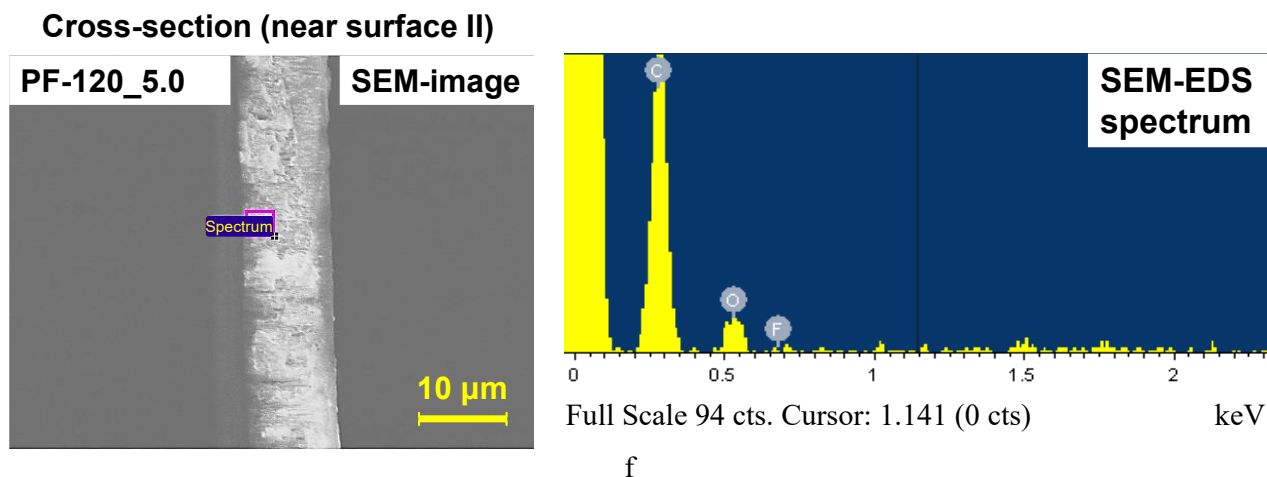


Figure S1. SEM-EDS spectrum and SEM images of SEM-EDS analysis areas of the surface TM120 substrate (a), surface I (b,c) and cross-section (near surface II) (d,f) of the experimental sample PF-543_2.5 and PF-120_5

S3. A microheterogeneous model algorithm for characterizing membrane structure and transport

The microheterogeneous model developed by Gnusin and co-authors [1–3] provides a quantitative framework for understanding how the structural and kinetic properties of a swollen ion-exchange membrane influence its transport characteristics, including transport numbers, sorption, diffusion permeability, and electrical conductivity. The model has been successfully applied to predict and describe the properties of various commercial and experimental ion-exchange membranes (IEM) [4,5] with diverse structures, including those doped with various dopants [6]. Also it can be applied to analysis of membrane behavior in solutions of strong and weak electrolytes [7] and studies of aging and fouling processes [8,9].

The model presents the ion-exchange membrane as a disordered microheterogeneous multiphase system. Using effective medium theory, it describes the overall physicochemical properties of the membrane as functions of the properties and relative positions of its constituent phases. In its simplest form, the microheterogeneous model represents the membrane as two pseudophases, distinguished by their conductivity mechanisms: a gel (or cluster) phase (f_1) and an intergel (or intercluster) phase (f_2). The gel phase is a quasi-homogeneous microporous medium comprising hydrophilic polymer chains of the ion exchanger with charged fixed groups, surrounded by a charged internal solution that compensates for the fixed group charge (the solution within the electrical double layer).

Within the gel phase, a distinction is often made between the hydrophilic region (“pure gel”) and a region of intertwined hydrophobic polymer chains lacking charged fixed groups. This hydrophobic region can consist of the reinforcing substrate or an inert binder. In the gel phase, current transfer ($\bar{\kappa}$) occurs solely via counterions (unipolar type of conductivity), with their movement limited by interactions with the fixed groups. In contrast, the intergel phase contains the internal equilibrium electrolyte solution, filling macroscopic membrane defects (cracks, caverns) and the central portions of mesopores (pores with radii $> 4\text{--}5\text{ nm}$). Current transfer in this phase (κ) is bipolar, involving both cations and anions. While ion movement in the intergel phase is less constrained, it remains dependent on the channel structure.

To simplify the analysis, the model incorporates several assumptions:

- The internal “intergel” solution possesses the same properties as the external equilibrium electrolyte solution;
- The gel phase and the intergel solution are in local equilibrium, as described by the Donnan equation;
- The electrolyte is completely dissociated;
- Ion-ion and ion-dipole interactions, as well as electroosmotic permeability, are considered negligible.

Based on the theory of generalized conductivity for structurally inhomogeneous materials and considering the assumptions above, the effective electrical conductivity (κ^* , under alternating current) of the ion-exchange membrane depends on both the conductivity of its individual phases and their spatial arrangement [3]:

$$\kappa^* = (f_1 \bar{\kappa}^\alpha + f_2 \kappa^\alpha)^{1/\alpha} \quad (\text{S1})$$

The structural parameter α describes the arrangement of phases within the membrane. A parallel arrangement of phases relative to the transport axis corresponds to $\alpha = 1$, while a series (or sequential) arrangement corresponds to $\alpha = -1$.

Equation (S1) can be simplified under specific conditions: when the structural parameter α approaches 0 ($|\alpha| \leq 0.2$, indicating a near-chaotic arrangement of conducting phases) and when the concentration of the external equilibrium solution is within an order of magnitude (no more than a factor of 10) of the isoelectric conductivity point (C_{iso}), where $\kappa^* = \bar{\kappa} = \kappa$:

$$\kappa^* = \bar{\kappa}^{f_1} \kappa^{f_2} \quad (\text{S2})$$

Linearization of equation (S2) in bilogarithmic coordinates allows us to determine the value of f_2 from the tangent of the slope of the straight line:

$$\lg \kappa^* = f_1 \lg \bar{\kappa} + f_2 \lg \kappa \quad (\text{S3})$$

$$f_2 = \frac{d \lg \kappa^*}{d \lg \kappa} \quad (\text{S4})$$

Next, using the expression $f_1 + f_2 = 1$, which determines the ratio of the conducting phases, we can find the proportion of the gel phase f_1 : $f_1 = 1 - f_2$. The linearity of the relationship (S3) in the given concentration range has been confirmed in several studies [10–12].

Outside the concentration range of $0.1 C_{iso} < C < 10 C_{iso}$, the slope of the $\lg(\kappa^*)$ vs. $\lg(\kappa)$ relationship increases with increasing external solution concentration [13]. At these higher concentrations, the membrane

conductivity becomes sensitive to the structural parameter α , which governs the relative contribution of the intergel phase to the overall membrane conductivity. When $\alpha \leq 0.2$ (indicating a dominant sequential connection of phases), the membrane conductivity is primarily limited by the less conductive gel phase. Conversely, when $\alpha \geq 0.2$ (indicating a dominant parallel connection), the more conductive intergel solution dictates the overall membrane conductivity. Consequently, as α increases, the membrane conductivity also increases, leading to a steeper slope in the $\lg(\kappa^*)$ vs. $\lg(\kappa)$ relationship. The slope reaches its maximum value for a free solution. When the $\lg(\kappa^*)$ vs. $\lg(\kappa)$ relationship deviates from linearity, the apparent volume fraction of intergel spaces, denoted as f_{2app} , is used to characterize the membrane. The value of f_{2app} increases with increasing concentration, reflecting the growing contribution of the intergel spaces to the membrane's overall conductivity. This effect is particularly significant in membranes with a high density of macropores filled with an electroneutral equilibrium solution.

At the isoelectric conductivity point, the electrical conductivity of the gel phase ($\bar{\kappa}$), can be approximated (neglecting the typically small contribution of co-ions) using the electrolyte's diffusion permeability coefficient in the gel phase \bar{D}_1 [14]:

$$\bar{\kappa} = \frac{z_1 \bar{D}_1 \bar{Q} F^2}{RT} \quad (S5)$$

$$\bar{Q} = \frac{Q}{f_1}, \quad (S6)$$

where \bar{Q} is the concentration of fixed ions in the gel phase, Q is the exchange capacity of the IEM, z_1 is the charge of the counterion, T is the temperature, R is the universal gas constant, F is the Faraday constant.

For more precise calculations, it is necessary to take into account that the conductivity of the gel phase also depends on the transport of co-ions in this phase (for 1:1 electrolyte):

$$\bar{\kappa} = (\bar{D}_1 \bar{c}_1 + \bar{D}_A \bar{c}_A) F^2 / RT \quad (S7)$$

where the concentrations of counterions and coions are found using the Donnan equation:

$$\frac{c^*}{c} = f_1 \frac{K_D}{Q} c + f_2 \quad (S8)$$

where, K_D is the Donnan constant, c^* is the concentration of co-ions sorbed per unit volume of the membrane $c^* = f_1 \bar{c}_A + f_2 c$.

Thus, at sufficiently low concentrations of the external solution, the ratio c^*/c should depend linearly on c , and the resulting straight line cuts off a segment on the ordinate axis equal to f_2 ; the tangent of the angle of inclination of the straight line is equal to $f_1 K_D / \bar{Q}$.

The differential (or “local”) diffusion permeability coefficient, P^* , is derived from the transfer equation within the framework of irreversible thermodynamics [3,15]. This local coefficient is related to the membrane's integral (or “global”) diffusion permeability coefficient, P , by the following expression [16]:

$$P^* = P \left(1 + \frac{d \lg P}{d \lg C} \right) = P(\beta + 1) \quad (S9)$$

where C is the electrolyte concentration (NaCl) ($C = |z_1|c_1 = |z_A|c_A$, index A denotes co-ion); β is parameter characterizing the concentration profile in the ion-exchange membrane [17].

Therefore, the differential diffusion permeability coefficient can be calculated from the experimentally determined concentration dependence of the integral diffusion permeability of the IEM.

Typically, for external equilibrium solution concentrations below 1 mol/L, the concentration of co-ions in the gel phase is inversely proportional to the concentration of fixed ions. This inverse proportionality allows for an approximate expression of the diffusion permeability using the following equation:

$$P^* = 2D_A t_1^* \left[f_1 \left(K_D \frac{\bar{D}_A c_A}{\bar{D}_A \bar{Q}} \right)^\alpha + f_2 \right]^{1/\alpha} \quad (S10)$$

Thus, the diffusion permeability of the membrane is controlled by the diffusion of co-ions in the gel phase and in the intergel spaces. The higher the values of the parameters f_2 and α , the higher the diffusion permeability of the membrane. In the first case, the diffusion of co-ions is determined by the Gnusin parameter [3,18]:

$$G = K_D \bar{D}_A / \bar{Q} D_A \quad (S11)$$

It characterizes the transport of co-ions in the gel phase of the membrane, i.e. reflects both the ability of the gel phase to sorb co-ions (ratio K_D / \bar{Q}) and the mobility of co-ions in this phase (ratio \bar{D}_A / D_A). Diffusion of electrolyte through the intergel phase is determined by the parameters f_1 (f_2), α and D_A . Thus, the greater

G, f_2 and α , the greater the diffusion permeability of the membrane. To find the above-described parameters of the model, the following algorithm was used in the work (similar to that proposed in [19]):

1. First, f_l and κ_{iso} are determined from the experimental relationship between the membrane's specific electrical conductivity and the concentration of the equilibrium solution. These data are analyzed in $\log \kappa_m - \log \kappa_{sol}$ coordinates. Next, f_2 is determined from the slope of this relationship using equation (S5); f_l is calculated using equation (S2).
2. The value of κ_{iso} is also determined from the coordinates of the intersection point between the concentration dependencies of the membrane conductivity and the conductivity of equilibrium solution.
3. The parameter β is determined from the concentration dependence of the diffusion flux, plotted in bilogarithmic coordinates, using equation (S9).
4. The differential diffusion permeability coefficient (P^*) is then calculated using equation (S9).
5. Using these previously determined values, α can be obtained from equation (S10).
6. Finally, G is calculated using equation (S11).

The values of κ^* and P^* obtained from the experiment allow us to determine the transport numbers of counterions (t_1^*) and co-ions (t_A^*) in the IEM using approximate equation [20]:

$$t_1^* = \frac{1}{2} + \sqrt{\frac{1}{4} - \frac{(z_1 |z_A|) P^* F^2 C}{(z_1 + |z_A|) R T \kappa^*}}, t_A^* = 1 - t_1^* \quad (S12)$$

Comparison of performances of LF-4SC pore-filled TM membrane PF-543_5 and previously reported different types of commercial and composite membranes fabricated from pore-filling method

Membranes	Membrane preparation (method, substrate/filling electrolyte)	Thickness _(dry) , μm	Exchange capacity _(dry) , mmol g^{-1}	Water content, $\text{g}_{\text{H}_2\text{O}} / \text{g}_{\text{dry}}$, %	¹ Resistance (Ohm cm^2)	t_{1app}^*	Ref.
Commercial membrane							
Nafion 117 (Du Pont)	melt extruding the sulfonyl fluoride precursor of PFSA	195	0.91	37	1.56	0.975 1/5 mM NaCl	[21]
CMX (ASTOM)	paste of PS+DVB+PVC	165	1.66	26.2	2.35	0.974 0.01/0.05 M KCl	[22]
CEM Type 1 (Fujifilm)	pore-filling, PO / AMPS+MBA	114	1.83	66.2	2.10	0.974 1/5 mM NaCl	[23]
Lab-made pore-filling membrane							
PF-543_5	PET TM / LF-4SC5	19	0.35	23.4	0.89	² 0.990	ours
PFPEM	PE / Sty95+DVB5	25	2.28	31.2	0.32	0.974 1/5 mM NaCl	[21]
PFCEM-4	PE / Sty65+GMA15	30	2.10	25.7	1.14	0.973 0.01/0.05 M KCl	[22]
PCEM	PE / AMPS	16	1.80	49.5	0.42	0.957 1/5 mM NaCl	[23]
SPES-PES	PES / SPES40	-	0.52	85.67	3	0.920 0.1/0.5 M KCl	[24]
PFCEM M	PTFE / SSS+MBA	35	1.97	49.79	-	0.910 0.01/0.05 M KCl	[25]
CEM	PO / crosslinked PESA	27	3.4	-	0.37	0.980 0.05/0.5 M NaCl	[26]
PFCEM-16T	PO / AMPS+BAP	20	1.75	-	0.36	0.940 0.01/1 M NaCl	[27]

¹ Membrane equilibrated with 0.5 M NaCl solution.

² the “true” counterion transport numbers, t_1^* , found from the conductivity and diffusion permeability measurements in 0.1 M NaCl solution.

DVB + PS is copolymer of polystyrene and divinylbenzene; PVC is polyvinyl chloride; PE is low-pressure polyethylene; PVDF is polyvinylidene fluoride; PET is polyethylene terephthalate; PFSA is perfluorosulfonic acid; AMPS is 2-acrylamido-2-methyl-1-propanesulfonic acid; MBA is *N,N'*-methylenebisacrylamide; GMA is glycidyl methacrylate; PES is poly (ether sulfone); SPES is sulfonated poly (ether sulfone); PTFE is polytetrafluoroethylene; SSS is sodium 4-vinylbenzenesulfonate; PO is polyolefin; BAP is *N,N*-bis(acryloyl)piperazine.

References

1. Gnusin, N. P., Berezina, N. P., Kononenko, N. A., & Dyomina, O. A. (2004). Transport structural parameters to characterize ion exchange membranes. *Journal of Membrane Science*, 243(1–2), 301–310. <https://doi.org/10.1016/j.memsci.2004.06.033>
2. Gnusin, N. P., Zabolotsky, V. I., Nikonenko, V. V., & Meshechikov, A. I. (1980). Development of the generalized conductance principle to the description of transfer phenomena in disperse systems under the acting of different forces. *Russian Journal of Physical Chemistry.*, 54, 1518–1522.
3. Zabolotsky, V. I., & Nikonenko, V. V. (1993). Effect of structural membrane inhomogeneity on transport properties. *Journal of Membrane Science*, 79(2–3), 181–198. [https://doi.org/10.1016/0376-7388\(93\)85115-D](https://doi.org/10.1016/0376-7388(93)85115-D)
4. Kamcev, J., Sujanani, R., Jang, E.-S., Yan, N., Moe, N., Paul, D. R., & Freeman, B. D. (2018). Salt concentration dependence of ionic conductivity in ion exchange membranes. *Journal of Membrane Science*, 547, 123–133. <https://doi.org/10.1016/j.memsci.2017.10.024>
5. Davydov, D., Nosova, E., Loza, S., Achoh, A., Korzhov, A., Sharafan, M., & Melnikov, S. (2021). Use of the microheterogeneous model to assess the applicability of ion-exchange membranes in the process of generating electricity from a concentration gradient. *Membranes*, 11(6), 406. <https://doi.org/10.3390/membranes11060406>
6. Porozhnyy, M., Huguet, P., Cretin, M., Safronova, E., & Nikonenko, V. (2016). Mathematical modeling of transport properties of proton-exchange membranes containing immobilized nanoparticles. *International Journal of Hydrogen Energy*, 41(34), 15605–15614. <https://doi.org/10.1016/j.ijhydene.2016.06.057>
7. Pismenskaya, N. (2001). Dependence of composition of anion-exchange membranes and their electrical conductivity on concentration of sodium salts of carbonic and phosphoric acids. *Journal of Membrane Science*, 181(2), 185–197. [https://doi.org/10.1016/S0376-7388\(00\)00529-9](https://doi.org/10.1016/S0376-7388(00)00529-9)
8. Porozhnyy, M. V., Sarapulova, V. V., Pismenskaya, N. D., Huguet, P., Deabate, S., & Nikonenko, V. V. (2017). Mathematical modeling of concentration dependences of electric conductivity and diffusion permeability of anion-exchange membranes soaked in wine. *Petroleum Chemistry*, 57(6), 511–517. <https://doi.org/10.1134/S0965544117060081>
9. Garcia-Vasquez, W., Dammak, L., Larchet, C., Nikonenko, V., Pismenskaya, N., & Grande, D. (2013). Evolution of anion-exchange membrane properties in a full scale electrodialysis stack. *Journal of Membrane Science*, 446, 255–265. <https://doi.org/10.1016/j.memsci.2013.06.042>
10. Sedkaoui, Y., Szymczyk, A., Lounici, H., & Arous, O. (2016). A new lateral method for characterizing the electrical conductivity of ion-exchange membranes. *Journal of Membrane Science*, 507, 34–42. <https://doi.org/10.1016/j.memsci.2016.02.003>
11. Manohar, M., Thakur, A. K., Pandey, R. P., & Shahi, V. K. (2015). Efficient and stable anion exchange membrane: Tuned membrane permeability and charge density for molecular/ionic separation. *Journal of Membrane Science*, 496, 250–258. <https://doi.org/10.1016/j.memsci.2015.08.051>
12. Nichka, V. S., Mareev, S. A., Porozhnyy, M. V., Shkirskaya, S. A., Safronova, E. Y., Pismenskaya, N. D., & Nikonenko, V. V. (2019). Modified microheterogeneous model for describing electrical conductivity of membranes in dilute electrolyte solutions. *Membranes and Membrane Technologies*, 1(3), 190–199. <https://doi.org/10.1134/S2517751619030028>
13. Sarapulova, V., Pismenskaya, N., Titorova, V., Sharafan, M., Wang, Y., Xu, T., Zhang, Y., & Nikonenko, V. (2021). Transport Characteristics of CJMAED™ Homogeneous Anion Exchange Membranes in Sodium Chloride and Sodium Sulfate Solutions. *International Journal of Molecular Sciences*, 22(3), 1415. <https://doi.org/10.3390/ijms22031415>
14. Helfferich, F. G. (1962). *Ion Exchange*. McGraw-Hill.
15. Kedem, O., & Katchalsky, A. (1963). Permeability of composite membranes. Part 3.—Series array of elements. *Trans. Faraday Soc.*, 59, 1941–1953. <https://doi.org/10.1039/TF9635901941>

16. Gnusin, N. P., Berezina, N. P., Shudrenko, A. A., & Ivina, A. P. (1994). Electrolyte diffusion across ion-exchange membranes. *Russian Journal of Physical Chemistry A*, 68, 506–510.
17. Berezina, N. P., Kononenko, N. A., Dyomina, O. A., & Gnusin, N. P. (2008). Characterization of ion-exchange membrane materials: Properties vs structure. *Advances in Colloid and Interface Science*, 139(1–2), 3–28. <https://doi.org/10.1016/j.cis.2008.01.002>
18. Gnusin, N. P., & Ivina, O. P. (1991). Diffusion of sodium chloride through an MK-40 cation-exchange membrane. *Russian Journal of Physical Chemistry A*, 65(9), 1299–1303.
19. V. I. Zabolotskii and V. V. Nikonenko, Ion Transport in Membranes (Nauka, Moscow, 1996) [in Russian]
20. Larchet, C., Dammak, L., Auclair, B., Parchikov, S., & Nikonenko, V. (2004). A simplified procedure for ion-exchange membrane characterisation. *New Journal of Chemistry*, 28(10), 1260. <https://doi.org/10.1039/b316725a>
21. Kim, D.-H., & Kang, M.-S. (2018). Water electrolysis using pore-filled proton-exchange membranes for hydrogen water production. *Chemistry Letters*, 47(10), 1265–1268. <https://doi.org/10.1246/cl.180560>
22. Kim, D.-H., Choi, Y.-E., Park, J.-S., & Kang, M.-S. (2019). Capacitive deionization employing pore-filled cation-exchange membranes for energy-efficient removal of multivalent cations. *Electrochimica Acta*, 295, 164–172. <https://doi.org/10.1016/j.electacta.2018.10.124>
23. Yang, S., Choi, Y.-W., Choi, J., Jeong, N., Kim, H., Nam, J.-Y., & Jeong, H. (2019). R2R Fabrication of Pore-Filling Cation-Exchange Membranes via One-Time Impregnation and Their Application in Reverse Electrodialysis. *ACS Sustainable Chemistry & Engineering*, acssuschemeng.9b01450. <https://doi.org/10.1021/acssuschemeng.9b01450>
24. Fan, H., Xu, Y., Zhao, F., Chen, Q.-B., Wang, D., & Wang, J. (2023). A novel porous asymmetric cation exchange membrane with thin selective layer for efficient electrodialysis desalination. *Chemical Engineering Journal*, 472, 144856. <https://doi.org/10.1016/j.cej.2023.144856>
25. Wang, B., Yan, J., Wang, H., Li, R., Fu, R., Jiang, C., Nikonenko, V., Pismenskaya, N., Wang, Y., & Xu, T. (2024). Solvent-free fabrication of pore-filling cation-exchange membranes for highly efficient desalination. *Chemical Engineering Science*, 287, 119782. <https://doi.org/10.1016/j.ces.2024.119782>
26. Akter, M., & Park, J.-S. (2023). Fouling and mitigation behavior of foulants on ion exchange membranes with surface property in reverse electrodialysis. *Membranes*, 13(1), 106. <https://doi.org/10.3390/membranes13010106>
27. Cha, J.-E., Seo, M. H., Choi, Y.-W., & Kim, W. B. (2021). A practical approach to measuring the ion-transport number of cation-exchange membranes: Effects of junction potential and analyte concentration. *Journal of Membrane Science*, 635, 119471. <https://doi.org/10.1016/j.memsci.2021.119471>